A high-quality factor hybrid plasmonic nanocavity based on distributed Bragg reflectors*

Linlin Tu(屠林林)[1], Chi Zhang(张弛)[1], Zhong Huang(黄忠)[1], Jason Yau[1,3], Peng Zhan(詹鹏)[1,2,†], and Zhenlin Wang(王振林)[1,2,‡]

[1] School of Physics and National Laboratory of Solid State Microstructures, Nanjing University, Nanjing 210093, China
[2] Collaborative Innovation Center of Advanced Microstructures, Nanjing 210093, China
[3] School of Physics, University of Western Australia, Perth WA 6009, Australia

(Received 25 March 2016; revised manuscript received 28 April 2016; published online 20 July 2016)

Herein, we propose a high-quality (Q) factor hybrid plasmonic nanocavity based on distributed Bragg reflectors (DBRs) with low propagation loss and extremely strong mode confinement. This hybrid plasmonic nanocavity is composed of a high-index cylindrical nanowire separated from a metal surface possessing shallow DBRs gratings by a sufficiently thin low-index dielectric layer. The hybrid plasmonic nanocavity possesses advantages such as a high Purcell factor (F_p) of up to nearly 20000 and a gain threshold approaching 266 cm^{-1} at 1550 nm, promising a greater potential in deep sub-wavelength lasing applications.

Keywords: plasmonic nanocavity, photonic crystal, nanowire

PACS: 73.20.Mf, 42.50.Pq, 81.07.Bc, 81.07.Gf **DOI:** 10.1088/1674-1056/25/9/097302

1. Introduction

Optical resonant cavities have attracted a great deal of attention because of their ability to manipulate optical energy in small volume and to consequently tailor light-matter interactions. This ability is of great importance, for it facilitates useful practical applications in designing optical filters, switches, low-threshold lasers, brighter single-photon sources, and so on.[1–9] Moreover, both confining the light in high-Q cavities to increase the lifetime of the optical excitation and reducing the effective mode volume ($V_{\rm eff}$) are crucial in the designs of the optical resonant cavities.[10]

Surface plasmon (SP) is the collective electron charge oscillations that exist at the interface between the metal and dielectric media. It is capable of producing highly enhanced optical fields below the diffraction limit, which yields great potential to confine and manipulate light at sub-wavelength scale with a reduced $V_{\rm eff}$.[11] As a result, recently, plasmonic resonators have been presented widely in theory and experiment, including diverse metallic nanocavities making use of localized SP (LSP)[12–15] and surface plasmon polaritons (SPPs).[10,16] However, the Q factors of LSP resonators are limited because of radiation and metallic losses. Although the SPPs resonators exhibit higher Q factors compared to LSP resonators, the former also suffer from huge propagation loss. In order to reduce propagation loss while offering tight mode confinement at sub-wavelength scale, a hybrid plasmonic waveguide comprised of a high-index dielectric nanowire separated from a silver surface by a nanoscale low-index dielectric gap was proposed,[17] which appears to be helpful in improving the Q factors of SPPs resonators. Subsequently, a plasmon laser[18] based on this kind of hybrid plasmonic waveguide was successfully demonstrated, and the feedback mechanism of this nanometer-scale plasmonic laser is based on a Fabry–Perot cavity provided by reflection of the nanowire end-facets. Taking into account the low reflection of the nanowire end-facets, we hope to further improve the Q factors of cavities by introducing high-reflectivity DBRs,[10,16] while maintaining a small mode volume.

In this letter, we design a hybrid plasmonic nanocavity based on DBRs, with an ultra-small mode volume and a high Q factor. As an example, Purcell factor of up to nearly 20000 and low gain threshold are achieved at 1550 nm, which are preferred to enable highly efficient nanocavity feedback for the potential applications such as deep sub-wavelength scale lasing.

2. Device model and numerical method

The proposed hybrid plasmonic nanocavity, as shown in Fig. 1(a), consists of a high-index GaAs nanowire separated from a Ag surface possessing shallow periodic gratings by a very thin low-index SiO_2 dielectric layer. The background is also made out of SiO_2 dielectric materials. The shallow periodic gratings serve as high-reflection DBRs, and two identical DBRs are placed along the direction of the GaAs nanowire

*Project supported by the National Key Basic Research Special Foundation of China (Grant Nos. 2012CB921501 and 2013CB632703) and the National Natural Science Foundation of China (Grant Nos. 11274160, 91221206, and 51271092).

†Corresponding author. E-mail: zhanpeng@nju.edu.cn
‡Corresponding author. E-mail: zlwang@nju.edu.cn

© 2016 Chinese Physical Society and IOP Publishing Ltd

with a selective distance between them to define a Fabry–Perot nanocavity, of which the length is L_1. The lengths between the cavity edge and its adjacent DBRs are defined as L_2, as shown in Fig. 1(a). The properties of this hybrid plasmonic nanocavity are investigated using COMSOL Multiphysics, a commercial finite-element-method-based software package. In our numerical simulations, the dielectric property of Ag is taken from Johnson & Christy[19] and the permittivities of GaAs and SiO_2 are set to be 12.25 and 2.25.

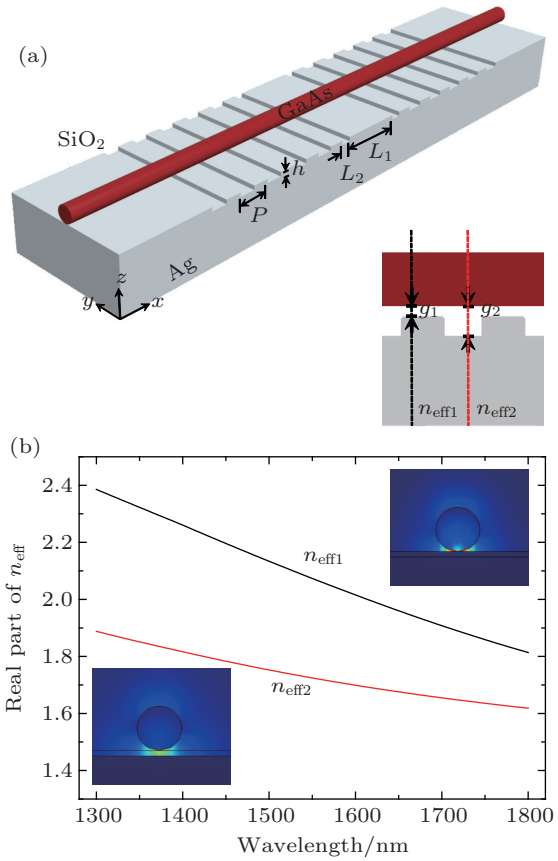


Fig. 1. (color online) (a) Schematic diagram of the hybrid plasmonic nanocavity, which comprises a high-index semiconductor nanowire separated from a patterned metal substrate by a nanoscale low-index dielectric gap. (b) Dependence of the real part of the effective refractive indices on the incident wavelength. The insets are the normalized electric field distributions in the yz plane corresponding to the two grating sub-period regions.

By controlling the hybridization of the fundamental guided mode of the 100 nm radius GaAs nanowire and the SPPs of the dielectric–metal interface at the telecommunication wavelength 1550 nm, we can simultaneously make sure tight mode confinement and single-mode propagation, as the dielectric gap width between the nanowire and the upper metal plane is set to $g_1 = 2$ nm. The depth of the grooves are set as $h = 25$ nm, in other words, $g_2 = g_1 + h = 27$ nm. The center wavelength of the stop band is related to the mode effective refractive indices. The mode effective refractive indices are calculated and displayed graphically in Fig. 1(b). It shows the real part of the effective refractive indices of the guided-mode propagating in the gap region between the GaAs cylinder and the metal surface with patterned grooves as a function of incident wavelength. Here, n_{eff1} and n_{eff2} are the effective refractive indices of the two-grating sub-period regions with gap widths of $g_1 = 2$ nm and $g_2 = 27$ nm, respectively. The normalized electric field intensity distributions of the hybrid plasmonic mode in the yz plane are shown in the insets of Fig. 1(b), corresponding to these two-gap widths, which clearly show that the hybrid plasmonic mode can be strongly confined in the gap region. In order to make sure the stop band is around 1550 nm, the grating period is designed to $P = 400$ nm and the width of the grooves are assumed as $P/2$ for simplicity.

3. Simulation results and discussion

The optical properties of the hybrid plasmonic nanocavities are subsequently investigated. In order to evaluate the propagation performance of the DBR, the transmission of a DBR grating composed of 10 periods with periodicity $P =$ 400 nm is simulated as plotted in the upper panel of Fig. 2(a). The incoming hybrid plasmonic mode tightly confined in the gap region between the patterned metal surface and nanocylinder is reflected with $> 99\%$ efficiency, thus forming a stop band with a bandwidth of 200 nm, ranging from 1500 nm to 1700 nm, which actually can be tuned by varying the grating period. A hybrid plasmonic nanocavity with length $L_1 =$ 770 nm can be constructed by placing two identical 5-period DBRs together for the defect state located around 1550 nm. The transmission spectra of the hybrid plasmonic nanocavities with different L_2 (the lengths between the cavity and its adjacent DBRs) are presented in the bottom panel of Fig. 2(a), in which there exist sharp resonant peaks located inside the stop band, and as L_2 increases, the resonant peaks red-shift obviously. In principle, a high-performance nanocavity can be scaled over a broad wavelength range for the target wavelength by optimizing the geometry of the nanostructure such as the parameters L_1 and L_2.

For example, when $L_2 = 126$ nm, a hybrid plasmonic nanocavity with resonant wavelength at 1550 nm can be achieved. Here, we use the ratio of the center wavelength of the resonant peak (λ_c) and its full width at half maximum (FWHM) to define the Q factor of this hybrid plasmonic cavity mode ($Q = \lambda_c/\text{FWHM}$). In this case, the transmittance of sharp resonant is 18.3% at $\lambda_c = 1550$ nm and the corresponding FWHM is 8.3 nm, which leads to a high Q factor of 187 owing to the low propagation loss. Since the transmission and FWHM of the resonant peak in the hybrid plasmonic nanocavity depend upon the period number (N) of the DBRs, as N increases, the FWHM reduces accordingly.[20,21] As an example, when the N of each DBR is 7 and 10, the FWHM reduces to about 5.3 and 4.6 nm, yielding higher Q factors of up to 292 and 337, respectively. However, as N increases, the decrease

of transmittance of the resonant peak will strongly limit the detection and its further application.[20,21] On the other hand, the mode volume of the proposed nanocavity can be calculated by

$$V_{\text{eff}} = \left[\iiint W(\boldsymbol{r})\,\mathrm{d}^3(\boldsymbol{r})\right]/W(\boldsymbol{r})_{\max}, \tag{1}$$

where $W(\boldsymbol{r})$ is the energy density, defined as

$$W(\boldsymbol{r}) = \frac{1}{2}\left[\mathrm{Re}\left[\frac{\mathrm{d}\{\varepsilon(\boldsymbol{r})\omega\}}{\mathrm{d}\omega}\right]|\boldsymbol{E}(\boldsymbol{r})|^2 + \mu\,|\boldsymbol{H}(\boldsymbol{r})|^2\right]. \tag{2}$$

When $L_2 = 126$ nm, an ultra-small mode volume of 3.04×10^{-22} m^3 can be achieved for the hybrid plasmonic nanocavity with length $L_1 = 770$ nm.

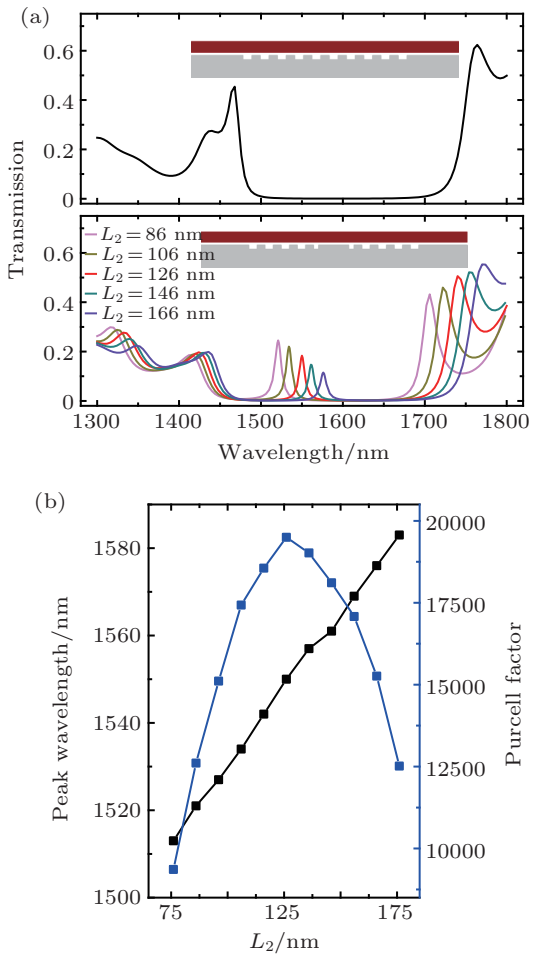


Fig. 2. (color online) (a) Transmission spectrum of a 10-period DBR (upper panel) and transmission spectra of hybrid plasmonic nanocavity composed of two 5-period DBRs with different L_2 (bottom panel). Insets are the schematics of each structure. (b) Dependence of the wavelength of the resonant peak and Purcell factor on the length L_2, varied from 76 nm to 176 nm at a step of 10 nm ($L_1 = 770$ nm).

Based on an overall consideration of the effect of Q factor and V_{eff} on the nanocavity, the Purcell factor is introduced to characterize the performance of the proposed nanocavity. Moreover, the Purcell factor is also a figure of merit to represent the ability of a cavity for spontaneous emission enhancement, which is described as[22]

$$F_{\text{p}} = \frac{3}{4\pi^2}\left(\frac{\lambda}{n_{\text{eff}}}\right)^3\left(\frac{Q}{V_{\text{eff}}}\right), \tag{3}$$

where λ is the resonance wavelength, Q is the quality factor, V_{eff} is the effective mode volume, and n_{eff} is the effective refractive index of the nanocavity. The wavelength of the resonant peak and Purcell factor as a function of L_2, are both shown in Fig. 2(b). With the increase of L_2 from 76 nm to 176 nm, the wavelength of the resonant peak shifts monotonically from 1513 nm to 1583 nm. It is noted that as L_2 is 126 nm, owing to the achievable high Q factor and ultra-small mode volume, the Purcell factor reaches its maximum value of 19498, a fairly high value compared with that of the nanocavities mentioned before.[10,15,22]

To illustrate the mode profile of the DBRs-based nanocavity clearly, the simulated normalized electric field intensity of the nanocavity in the xy plane at different wavelengths are plotted in Fig. 3. Here, for the proposed sample $L_2 = 126$ nm, the hybrid plasmonic mode propagating characteristics for wavelengths at 1600 nm, 1740 nm, and 1550 nm are presented, which correspond to three typical wavelengths including inside the stop band, outside the stop band, and on resonance, due to the excitation of cavity mode, respectively. As shown in Fig. 3(b) at wavelength $\lambda = 1600$ nm, we observe that the light is reflected after a couple of periods inside the stop band. Moreover, the light propagates through the structure at wavelengths outside the stop band, as shown in Fig. 3(c), when the wavelength is at 1740 nm. Figure 3(d) shows that at $\lambda = 1550$ nm, the incident light couples and strongly resonances in the nanocavity.

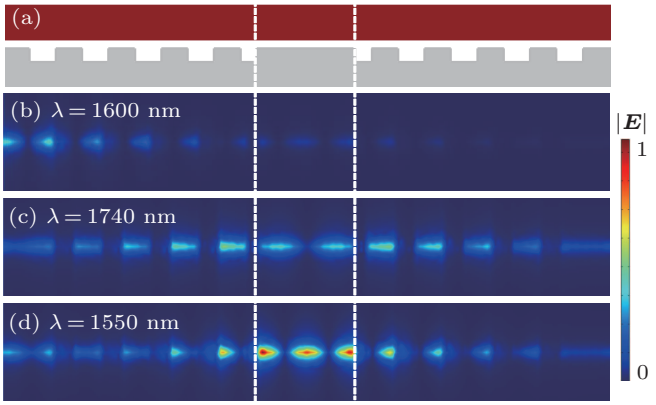


Fig. 3. (color online) (a) Schematic diagram of the hybrid plasmonic nanocavity. Simulated normalized electric field intensity from the xy plane at the middle of the dielectric gap of hybrid plasmonic nanocavities at (b) $\lambda = 1600$ nm (inside the stop band), (c) $\lambda = 1740$ nm (outside the stopband), and (d) $\lambda = 1550$ nm (on resonance).

Due to the large Purcell factor, which represents the fine ability of the hybrid plasmonic nanocavity for spontaneous emission enhancement that was demonstrated in plasmonic nanoparticle antennas,[23] we also demonstrate the utility of

the hybrid plasmonic nanocavity to control emission properties of dipole for the optimized $L_2 = 176$ nm at wavelength of 1550 nm. Figure 4(a) shows simulated photoluminescence (PL) intensity spectra of x-, y-, and z-polarized dipole sources being placed at the center of our proposed DBRs-based hybrid plasmonic nanocavity. The PL intensity of z-polarized dipole source coupled to the cavity is much higher than that of x- and y-polarized one. This is because E_z is about three orders of magnitude higher than E_x and E_y at this point. The resonance peak of PL intensity spectrum of z-polarized dipole λ is 1550 nm, which corresponds well with transmission spectra of the cavity. Figures 4(b)–4(d) show E_x, E_y, and E_z distributions in the yz plane of the cavity without dipole at $\lambda = 1550$ nm, respectively. The electric field distributions also reveal that E_z is much higher than E_x and E_y.

Considering the relatively high Q factor and ultra-small mode volume of the hybrid plasmonic nanocavity, we expect a low gain threshold for the lasing applications. To find out the gain threshold, a nanowire is chosen to be doped with optical gain material and we set the complex permittivity of the GaAs as $\varepsilon_g(\varepsilon_g = \varepsilon'_g + i\varepsilon''_g = 12.25 + i\varepsilon''_g)$. We then calculate the absorption efficiency for the hybrid plasmonic nanocavity with different gain coefficient $\alpha\left(\alpha = (2\pi/\lambda)\,\mathrm{Im}(\varepsilon'_g + i\varepsilon''_g)^{1/2}\right)$. The zero absorption at a critical value, i.e., the gain threshold, means that loss in metal has been totally compensated by the gain in the nanowire. As a result, the gain threshold α_{th} for the hybrid plasmonic nanocavity with $L_2 = 126$ nm is calculated to be 266 cm^{-1}, much smaller than that of the recently reported plasmonic lasing structures.[22,24]

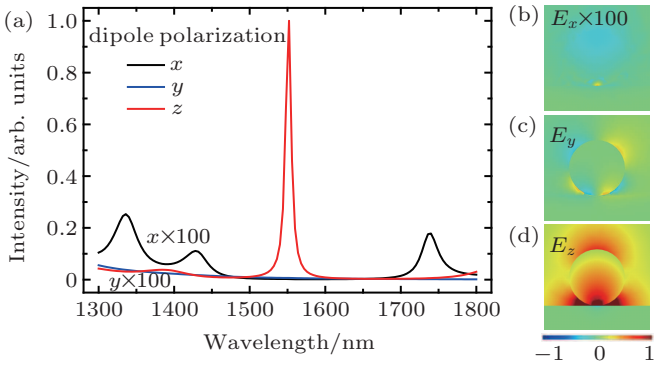


Fig. 4. (color online) (a) Simulated PL intensity spectra for x- (black line), y- (blue line), and z-polarized (red line) dipole sources placed at the center of cavity with $L_2 = 126$ nm. (b)–(d) E_x, E_y and E_z distributions in the yz plane of the cavity without dipole at the center of the cavity respectively.

4. Conclusion and perspectives

We design a hybrid plasmonic nanocavity with high Q factor and ultra-small mode volume based on the DBRs and the hybrid plasmonic waveguide. The characteristics of Purcell factor of up to nearly 20000 and low gain threshold approaching 266 cm^{-1} at the telecommunication wavelength 1550 nm provide efficient cavity feedback and high lasing efficiency. This result shows significant potential for subwavelength lasing applications and development of nanoscale integrated photonic circuits

References

[1] Noda S, Fujita M and Asano T 2007 *Nat. Photon* **1** 449
[2] Bianucci P, Wang X, Veinot J G and Meldrum A 2010 *Opt. Express* **18** 8466
[3] Yanik M F, Fan S and Soljacic M 2003 *Appl. Phys. Lett.* **83** 2739
[4] Robinson J T, Christina M, Long C and Michal L 2005 *Phys. Rev. Lett.* **95** 143901
[5] Vahala K J 2003 *Nature* **424** 839
[6] Wiersig J and Hentschel M 2006 *Phys. Rev. A* **73** 031802
[7] Akimov A V, Mukherjee A, Yu C L, Chang D E, Zibrov A S, Hemmer P R, Park H, and Lukin M 2007 *Nature* **450** 402
[8] Kolesov R, Grotz B, Balasubramanian G, Stöhr R J, Nicolet A A L, Hemmer P R, Jelezko F and Wrachtrup J 2009 *Nat. Phys.* **5** 470
[9] Chang D E, Sørensen A S, Hemmer P R and Lukin M D 2006 *Phys. Rev. Lett.* **97** 053002
[10] de Leon N P, Shields B J, Yu C L, Englund D E, Akimov A V, Lukin M D and Park H 2012 *Phys. Rev. Lett.* **108** 226803
[11] Gramotnev D K and Bozhevolnyi S I 2010 *Nat. Photonics* **4** 83
[12] Hill M T, Oei Y S, Smalbrugge B, Zhu Y, de Vries T, van Veldhoven P J, van Otten FWM, Eijkemans T J, Turkiewicz J P, de Waardt H, Geluk E J, Kwon S H, Lee Y H, Nötzel R and Smit M K 2007 *Nat. Photonics* **1** 589
[13] Noginov M A, Zhu G, Belgrave A M, Bakker R, Shalaev V M, Narimanov E E, Stout S, Herz E, Suteewong T and Wiesner U 2009 *Nature* **460** 1110
[14] Pan J, Chen Z, Chen J, Zhan P, Tang C J and Wang Z L 2012 *Opt. Lett.* **37** 1181
[15] Xiao Y, Liu Y, Li B, Chen Y, Li Y and Gong Q 2012 *Phys. Rev. A* **85** 031805
[16] Jiang H, Liu C, Wang P, Zhang D, Lu Y and Ming H 2013 *Opt. Express* **21** 4752
[17] Oulton R F, Sorger V J, Genov D A, Pile D F P and Zhang X 2008 *Nat. Photonics* **2** 496
[18] Oulton R F, Sorger V J, Zentgraf T, Ma R M, Gladden C, Dai L, Bartal G and Zhang X 2009 *Nature* **461** 629
[19] Johnson P B and Christy R W 1972 *Phys. Rev. B* **6** 4370
[20] Xu C, Hu T, Chen R, Ping Y, Yang J and Jiang X 2013 *J. Opt* **15** 105005
[21] Xiao J, Liu J, Zheng Z, Bian Y, Wang G and Li S 2012 *Phys. Status Solidi A* **209** 1552
[22] Xiang C, Chan C K and Wang J 2014 *Sci. Rep.* **4** 3720
[23] Chen X, Agio M and Sandoghdar V 2012 *Phys. Rev. Lett.* **108** 233001
[24] Li Z, Piao R, Zhao J, Meng X and Tong K 2015 *Chin. Phys. B* **24** 077303